

EFFECTS OF MACROMOLECULAR CROWDING ON FOLDING OF SMALL GLOBULAR PROTEINS

NHUNG T. T. NGUYEN^{1,2}, PHUONG THUY BUI^{3,4} AND TRINH XUAN HOANG^{1,2,†}

¹*Institute of Physics, Vietnam Academy of Science and Technology,
10 Dao Tan, Ba Dinh, Hanoi 11108, Vietnam*

²*Graduate University of Science and Technology, Vietnam Academy of Science and Technology,
18 Hoang Quoc Viet, Cau Giay, Hanoi 11307, Vietnam*

³*Institute of Theoretical and Applied Research,
Duy Tan University, Hanoi, 100000, Vietnam*

⁴*Faculty of Pharmacy, Duy Tan University, Da Nang, 550000, Vietnam*

E-mail: [†]txhoang@iop.vast.vn

Received 17 December 2021; Accepted for publication 13 April 2022; Published 21 May 2022

Abstract. *The effects of inert spherical crowders on the melting temperature and the folding stability of small globular proteins are investigated by using molecular dynamics simulations with a Gō-like model for the proteins. The energy parameter in the Gō-like model is obtained individually for each protein by matching the models melting temperature to the experimental melting temperature in the absence of crowders. It is shown that both the melting temperature and the folding stability of protein increase in the presence of the crowders. Specifically, as the crowders volume fraction ϕ_c increases from 0 to 0.4 the melting temperature increases by more than 20 Kelvins, whereas the folding stability is enhanced by up to ~ 3.6 kcal/mol depending on the protein and the temperature. At room temperature (300 K), the stability enhancement is 1.2–1.4 kcal/mol, which is close to prior experimental data. It is also shown that the dependence of the folding free energy change on ϕ_c can be fitted well to the scaled particle theory by assuming a linear dependence of the effective size of the unfolded state on ϕ_c .*

Keywords: MD simulation, folding stability, scaled particle theory.

Classification numbers: 87.15.M-; 87.64.K- .

I. INTRODUCTION

Macromolecular crowding, the condition typically referring to the cytoplasm which is populated by high concentrations of macromolecules, is known to influence the equilibria and rates of many cellular reactions including protein folding [1–3]. It has been shown that macromolecular crowding enhances the native state's stability and the folding rates of proteins [4, 5], and promotes

protein aggregation [6, 7]. Theoretical models based on the scaled particle theory (SPT) [8–10] have been very useful for interpreting and quantifying the effects of macromolecular crowding on protein stability. The available models, however, still need thorough quantitative comparisons with experiment [5, 11].

The primary effect of crowding on protein stability is due to the excluded volume of crowders, which affects the unfolded state much stronger than the folded state resulting in an enhancement of the native state's stability. In the SPT model of Minton [8], the stability enhancement is obtained by considering both the unfolded state and the folded state as effective hard spheres of specified radii. Minton's model is supported by simulations of proteins with spherical crowders, which showed that the stability increase is ranged up to 2–5 kcal/mol at room temperatures [12]. Experiments on folding using synthetic crowders showed that they have only a modest stabilizing effect, of 0.5–1.2 kcal/mol, on the protein's folded state [13, 14].

In a recent work [15], we have shown that the fit of SPT to simulation data is significantly improved by considering the effective radius of the unfolded state to be a linear function of the crowders' volume fraction ϕ_c . The aim of the present study is to get quantitative estimates of the effects of crowders on the melting temperature and the folding stability of proteins by simulations, and to check if the SPT works at various interested temperatures. For this purpose, we employed a working protein model whose the energy parameter is determined individually for each protein by fitting the temperature of the specific heat's peak with the experimental melting temperature for the case without crowders. The model, therefore, has a correct energy scale for each protein, allowing quantitative results to be obtained in the simulations with crowders.

II. METHODS

Protein and crowder models

We consider two proteins of different classes of native state topology: a β -sheet protein, the Src-Homology (SH3) domain, and an α -helical protein, the chicken's villin headpiece (HP67) domain whose the chain lengths are 57 and 67 amino acids, respectively. The native conformations of these proteins are shown in Fig. 1 (a and b) with the corresponding protein data bank (PDB) codes 1SHG and 2RJX, respectively. For convenient, we denote the proteins by their PDB codes. The proteins are considered in the off-lattice Gō-like model of Clementi *et al.* [16], which follows the early lattice model by Gō [17]. Each amino acid residue is represented by a single bead centered at the position of the alpha carbon (C_α) atom. The potential energy of a protein in a given conformation is

$$E = \sum_i K_b (r_{i,i+1} - r_{i,i+1}^*)^2 + \sum_i K_\theta (\theta_i - \theta_i^*)^2 + \sum_{n=1,3} \sum_i K_\phi^{(n)} [1 + \cos(\phi_i - n\phi_i^*)] \\ + \sum_{i < j+3}^{\text{native}} \epsilon \left[5 \left(\frac{r_{ij}^*}{r_{ij}} \right)^{12} - 6 \left(\frac{r_{ij}^*}{r_{ij}} \right)^{10} \right] + \sum_{i < j+3}^{\text{non-native}} \epsilon \left(\frac{\sigma}{r_{ij}} \right)^{12}, \quad (1)$$

where r_{ij} is the distance between bead i and bead j ; θ_i and ϕ_i are the bond and dihedral angles of residue i , respectively; the star corresponds to the native state values; ϵ is an energy parameter corresponding to the depth of the 10-12 Lennard-Jones (LJ) potential for native contacts; $\sigma = 5 \text{ \AA}$ represents an effective diameter of amino acid; $K_b = 100\epsilon$, $K_\theta = 20\epsilon$, $K_\phi^{(1)} = -\epsilon$, and $K_\phi^{(2)} = -0.5\epsilon$. The last two terms in Eq. (1) correspond to summations over native and non-native contacts,

respectively. Native contacts are determined based on an all-atom consideration of the protein's native state given by the PDB structure. A native contact between two amino acid residues is defined if they have at least two heavy atoms within a distance smaller than 4.5 Å.

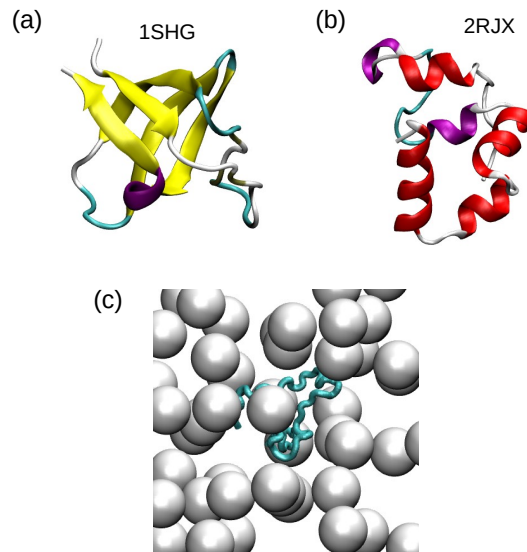


Fig. 1. Native state conformations of the SH3 domain (PDB ID: 1SHG) (a) and the HP67 headpiece domain of chicken villin (PDB ID: 2RJX) (b). (c) Snapshot of a simulated system of an unfolded protein surrounded by spherical crowders.

The parameter ϵ in Eq. (1) represents an average energy of all native contacts of a protein in its native state. Following Ref. [18], the value of ϵ is determined for each protein by matching the temperature of the specific heat's peak T_m^* obtained by the simulations with the experimental melting temperature T_m^{exp} of the protein. Specifically, from simulations of isolated proteins (without crowders) in reduced units we obtained $T_m^* = 1.075 \epsilon/k_B$ for 1SHG and $T_m^* = 0.912 \epsilon/k_B$ for 2RJX. Given that $T_m^{exp} = 82^\circ\text{C}$ for 1SHG [19] and $T_m^{exp} = 81^\circ\text{C}$ for 2RJX [20], one obtains $\epsilon = 0.656$ kcal/mol for 1SHG and $\epsilon = 0.771$ kcal/mol for 2RJX.

The crowders are modelled as soft spheres of radius $R_c = 10$ Å, which is roughly the sizes of the two proteins considered. All amino acids are assumed to have the same mass $m = 120$ g/mol, whereas the mass of crowder is chosen to be $m_c = 56m$, equal to the weight of a small protein [15]. The interactions between an amino acid and a crowder and between two crowders are given by a truncated and shifted LJ potential with the use of virtual residues as introduced in our previous works [15, 21].

Simulation method

Molecular Dynamics (MD) method based on the Langevin equation and a Verlet algorithm [22] is employed to simulate the dynamics of the proteins and the crowders (see also Ref. [15] for more details). For a given crowder volume fraction ϕ_c , the simulated system typically consists of one protein and multiple crowders in a cubic box of size $L = 100$ Å with periodic

boundary conditions (Fig. 1(c)). We also employed the replica-exchange MD method [23] to improve equilibrium sampling. In this method, one simulates multiple copies (or replicas) of a system under equilibrium conditions at various temperatures by parallel MD simulations and regularly attempts swap moves that exchange the replica conformations at neighboring temperatures with appropriate velocity rescaling. The exchange probability is chosen such that it maintains the detailed balance condition at each temperature [24]. For a given system of protein and crowders, 10–12 replicas were simulated at a range of temperatures that spans from above to below the folding transition of the protein. Swap moves were attempted every 10τ , where $\tau = \sqrt{m\sigma^2/\epsilon}$ is a reduced time unit. The replica temperatures were adjusted several times in subsequent simulations so that the acceptance rates of swap moves are higher than 0.2 for all pairs of neighboring temperatures. The typical length of a simulation is $10^6\tau$.

Equilibrium properties of proteins, such as the specific heat, the free energy, are obtained from the simulation data with the help of the weighted multiple histogram analysis method [25]. The free energy is determined as a function of the fraction of native contacts Q as $F(Q) = -k_B T \ln P(Q)$, where k_B is the Boltzmann's constant, T is the absolute temperature, and $P(Q)$ is the probability of observing conformations with the fraction of native contacts Q . The folding free energy (ΔF_{N-U}) of a protein is defined as the free energy difference between the native state (N) and the unfolded state (U) and is calculated as [12]

$$\Delta F_{N-U} = F_N - F_U = -k_B T \ln \left(\frac{\int_{Q_{\ddagger}}^1 e^{-\beta F(Q)} dQ}{\int_0^{Q_{\ddagger}} e^{-\beta F(Q)} dQ} \right), \quad (2)$$

where Q_{\ddagger} denotes the value of Q at the transition state (\ddagger). The folding free energy change ($\Delta\Delta F_{N-U}$) due to macromolecular crowding is defined as

$$\Delta\Delta F_{N-U} \equiv \Delta F_{N-U}(\phi_c) - \Delta F_{N-U}(0). \quad (3)$$

Scaled particle theory

In the scaled particle theory (SPT), the Helmholtz free energy change of inserting a hard sphere particle of radius R in a fluid of hard sphere crowders of radius R_c is given by [26]

$$\frac{\Delta F}{k_B T} = -\ln(1 - \phi_c) + \rho y(3 + 3y + y^2) + \rho^2 y^2(9/2 + 3y) + 3\rho^3 y^3, \quad (4)$$

where ϕ_c is the volume fraction of crowders, $\rho = \phi_c/(1 - \phi_c)$, and $y = R/R_c$. By considering the folded state and unfolded state of a protein as effective hard spheres of radii a_N and a_U , respectively, the folding free energy change due to the presence of crowders can be calculated [8]. In the present study, a_N is chosen to be equal to the radius of gyration of the native conformation, whereas a_U is considered as a linear function of ϕ_c [15]. The explicit form of function for a_U is obtained by fitting the SPT model to the simulation data.

III. RESULTS AND DISCUSSION

We carried out the simulations for the two proteins, 1SHG and 2RJX, at 4 different crowders' volume fractions, $\phi_c = 0, 0.1, 0.2, 0.3$ and 0.4 , and calculated the specific heat as a function of temperature and the free energy as a function of the fraction of native contacts, Q , for all cases. Note that the volume fraction of 0.4 is close to real conditions of cytoplasm. The acceptance rates of attempted swap moves in our replica-exchange MD simulations are in the range from

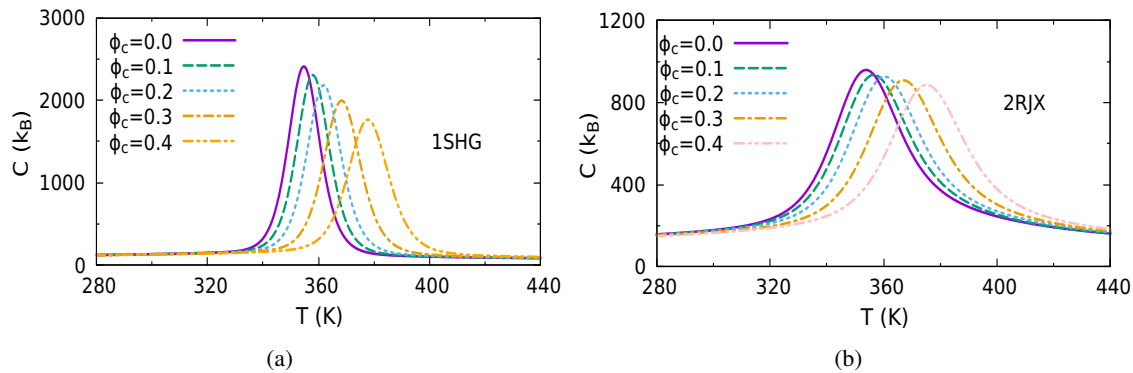


Fig. 2. Temperature dependence of the specific heat for protein 1SHG (a) and protein 2RJX (b) at different crowders' volume fraction $\phi_c = 0, 0.1, 0.2, 0.3$ and 0.4 as indicated.

0.22 to 0.84, ensuring sufficient statistics. Figure 2 shows that for both proteins, as ϕ_c increases the melting temperature T_m , defined as the temperature of the specific heat's peak, also increases, indicating that the proteins are thermally more stable under a higher crowder concentration. The height of the specific heat's peak is found to decrease with ϕ_c indicating the cooperativity [27] of the folding transition is decreased. Note also that the specific heat's peak of 2RJX is substantially lower than that of 1SHG. Fig. 3 shows that the stability enhancements are similar for both proteins with T_m increased by more than 20 degrees as ϕ_c is changed from zero to 0.4. Note also that the increase in T_m with ϕ_c is slightly non-linear for both proteins with a faster increase at a higher ϕ_c (Fig. 3).

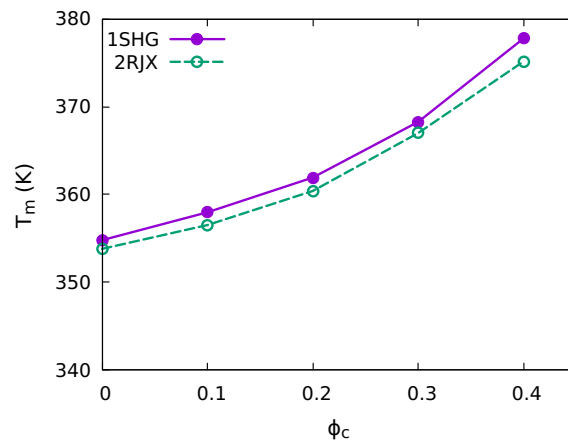


Fig. 3. Dependence of the melting temperature T_m on the crowders' volume fraction ϕ_c for protein 1SHG (filled circles) and protein 2RJX (open circles).

Figure 4 shows that the typical MD trajectories at the melting temperature for 1SHG for both cases, in the absence (Fig. 4a) and in the presence of crowders (Fig. 4b), have multiple switchings between low and high energy conformations corresponding to the folded and unfolded

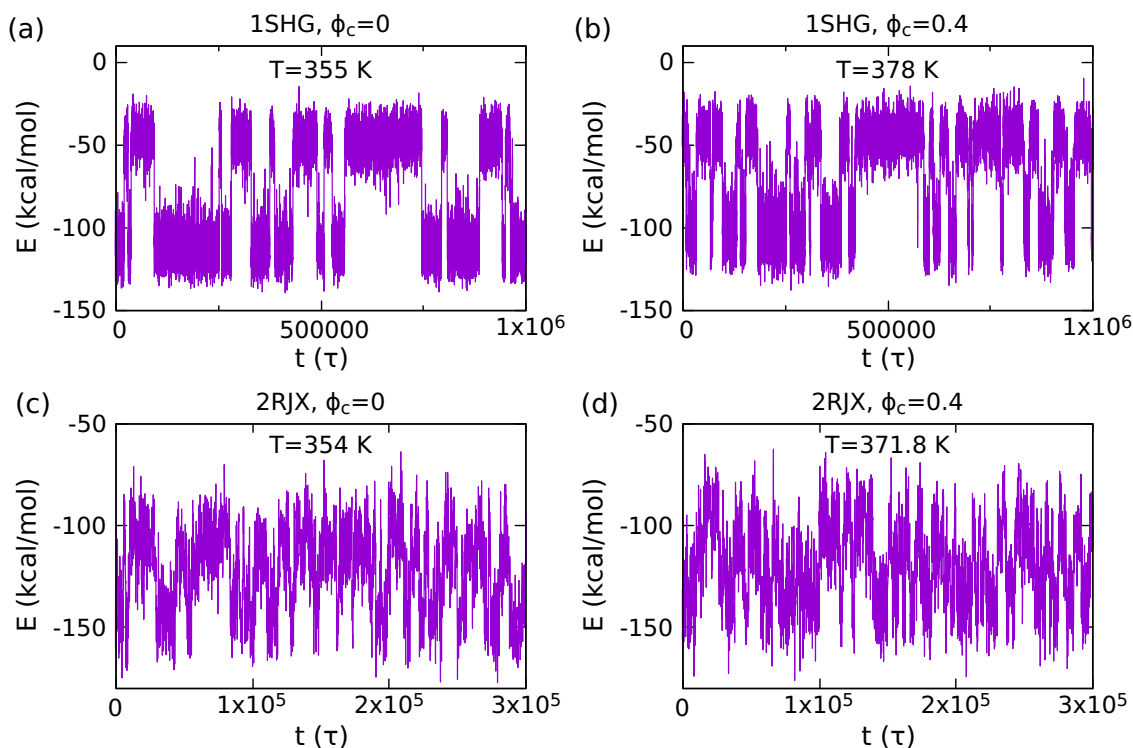


Fig. 4. Time dependences of the energy of protein 1SHG (a,b) and protein 2RJX (c,d) in long simulations at their melting temperatures in the absence of crowders ($\phi_c = 0$) (a,c) and in the presence of crowders with $\phi_c = 0.4$ (b,d).

states of the protein, respectively. This result indicates that the folding mechanism is two-state and that the crowding condition does not change the folding mechanism of the protein. However, it can be noticed that the switching frequency increases on changing from $\phi_c = 0$ (Fig. 4a) to $\phi_c = 0.4$ (Fig. 4b), suggesting that the crowding decreases the folding free energy barrier. For protein 2RJX, the trajectories (Fig. 4 (c and d)) show that folding mechanism is also two-state but not as clear as for 1SHG, and the effect of the crowders on the switching frequency between the low and high energy conformations is not clearly seen. It is indicated that the crowders have a smaller effect on the folding barrier of 2RJX than for 1SHG.

Figure 5 shows the dependence of the free energy F on the fraction of native contacts, Q , for the two proteins at different values of ϕ_c . The free energy profiles are obtained at the experimental melting temperature of each protein. For most cases, the free energy has two minima corresponding to the folded and unfolded states. For comparison, we have fixed the free energy of the folded state (the minimum of F at high Q value) to be equal to zero as the effect of crowders on the folded state is expected to be much smaller than on the unfolded state. Fig. 5 shows that for both proteins, as ϕ_c increases, the free energy difference between the unfolded state and the folded state also increases indicating enhancement of the folding stability. Fig. 5b also shows that for protein 2RJX the minimum of F at low Q values disappears at $\phi_c > 0.2$ suggesting that the

unfolded state of this protein is completely destabilized at high concentrations of crowders at the given temperature.

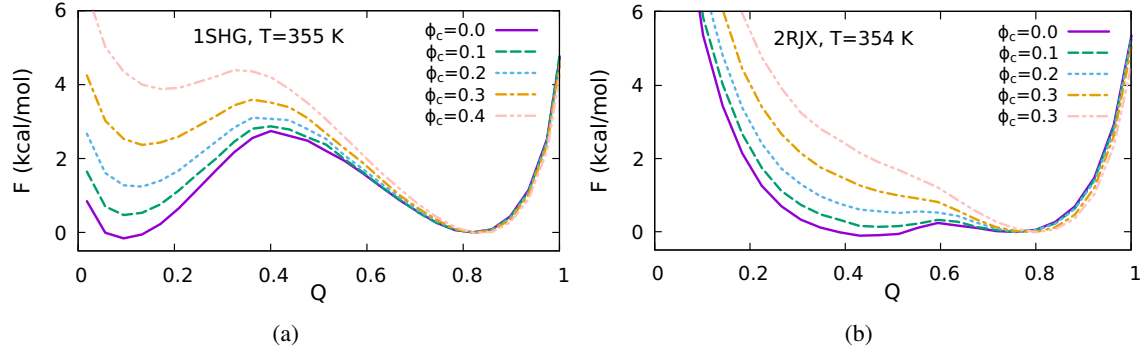


Fig. 5. Dependence of the free energy F on the fraction of native contacts, Q , at the experimental melting temperature, $T = 355$ K for protein 1SHG (a) and $T = 354$ K protein 2RJX (b). The lines shown correspond to different values of the crowder volume fraction ϕ_c as indicated.

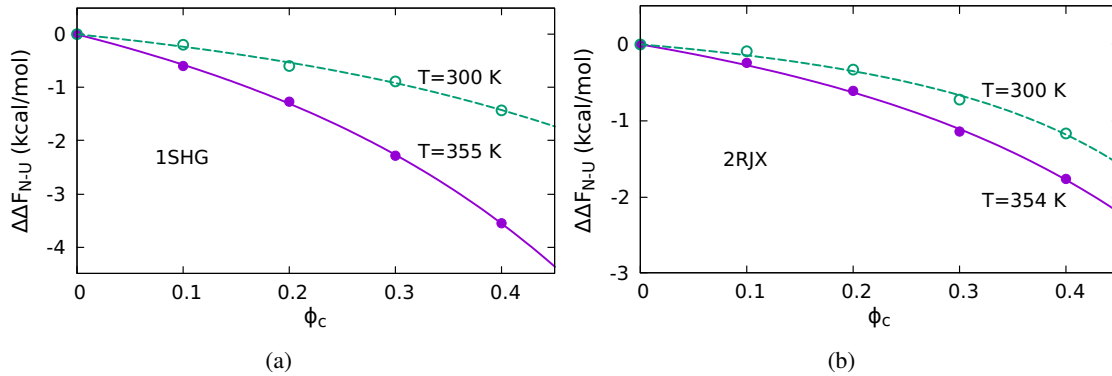


Fig. 6. Dependence of the folding free energy change, $\Delta\Delta F_{N-U}$, on the crowder volume fraction, ϕ_c , obtained by simulations for 1SHG (a) and 2RJX (b) at their experimental melting temperatures, $T = 355$ K for 1SHG and $T = 354$ K for 2RJX, (filled circles) and at $T = 300$ K (open circles) as indicated. The associated solid and dashed lines show the fits of the scaled particle theory to the simulation data.

We turn now to the fitting of simulation data to the scaled particle theory model. The folding free energy changes in the simulations were calculated from the free energy profiles using Eqs. (2) and (3). Following previous work [15], we applied the SPT with a_N equal the radius of gyration of the protein native state whereas a_U is considered as a linear function of ϕ_c (the parameters of this linear function are obtained by the fitting). Fig. 6 shows that the folding free energy change can be fitted very well by the SPT for both proteins at their experimental melting temperatures T_m^{exp} and at

the room temperature $T = 300$ K, indicating that the linear function of ϕ_c is a correct form of a_U . Fig. 6 also shows that the change in the folding free energy due to the crowding is much stronger for 1SHG than for 2RJX, and for each protein it is much stronger at the melting temperature than at the room temperature. Particularly, at the highest crowders' volume fraction, $\phi_c = 0.4$, the free energy change for 1SHG is about 3.56 kcal/mol at $T = 355$ K and 1.43 kcal/mol at $T = 300$ K. The corresponding values for 2RJX are 1.77 kcal/mol at $T = 354$ K and 1.17 kcal/mol at $T = 300$ K. Table 1 shows that the linear function for a_U obtained from the fitting depends on the protein and on the temperature. Similar to the folding free energy change, the dependence of a_U on ϕ_c is stronger for 1SHG than for 2RJX, and is stronger at the experimental melting temperature than at the room temperature.

Table 1. The parameters a_N and a_U used in the fits the simulation data shown in Fig. 6 to the scaled particle theory. Note that a_U is considered as a linear function of ϕ_c .

Protein	T (K)	a_N (Å)	a_U (Å)
1SHG	355	9.63	$14.23 - 5.91 \phi_c$
1SHG	300	9.63	$12.11 - 3.32 \phi_c$
2RJX	354	11.0	$13.78 - 3.52 \phi_c$
2RJX	300	11.0	$12.73 - 1.59 \phi_c$

Experimentally, it has been shown that Ficoll 70, an inert spherical crowding agent, has a strong effect on the thermal stability of the 148-residue single-domain protein apoflavodoxin with T_m increased by 20°C at the highest Ficoll concentration of 400 g/L and pH 7 [5]. Ficoll 70 was also shown to increase the folding stability of the 81-residue protein FKBP12 by ~ 0.5 kcal/mol at the crowder concentration of 180 g/L [13]. Another experiment showed that at 37°C the 76-residue wild-type ubiquitin is stabilized by 1.2 kcal/mol at 150 g/L of dextran, another type of inert crowding agent [14]. It appears that our simulations, though performed on different proteins, yield the thermal and folding stability enhancements close to these experimental results.

There has been no clear indication about whether the stabilizing effect of crowders on proteins depends on the protein size. On the other hand, it has been shown that this effect depends strongly on the crowder size, by both theory and experiment (see e.g. [12, 28]). At the same crowders' volume fraction, the smaller the crowder, the stronger the effect. In this study, we have considered a relatively small size of the crowders, of the radius of 10 Å, which is about the sizes of the smallest globular proteins. Thus, the obtained stability enhancements (~ 20 K in melting temperature and ~ 1.4 kcal/mol in the folding free energy) would correspond to the strongest effects under cellular crowding conditions. Note that the effect also varies with the protein and with the macromolecular volume fraction in cells, for which ϕ_c can vary from 0.3 to 0.4. Even though the stabilizing effect of macromolecular crowding on proteins seems to be modest, it may be utilized by proteins whose function is sensitive to thermal stability. For example, it is known that the activity of the G6PD enzyme is coupled to the thermal stability of this enzyme [29].

IV. CONCLUSION

In this work, we have studied the effects of macromolecular crowding on the thermal stability and the folding stability of two small proteins of different classes of the native state conformation. We have shown that despite the difference in the native state topology, the increases in the melting temperature are similar for both proteins and are up to about 21–23 K on changing the crowders' volume fraction ϕ_c from 0 to 0.4. On the other hand, the effect of crowders on the folding stability strongly depends on the protein and on the temperature. For the β -sheet protein 1SHG the folding free energy change is stronger than for the α -helical protein 2RJX. At $\phi_c = 0.4$, the stability enhancements are found to be ~ 1.8 – 3.6 kcal/mol at the experimental melting temperatures (354–355 K), whereas it is only about 1.2–1.4 kcal/mol at room temperature (300 K). These results to some extent quantitatively agree with prior experimental data, which showed that the melting temperature of protein can increase by 20 K at a high crowder concentration [5] and stability enhancement is about 0.5–1.2 kcal/mol [13, 14]. The present study also shows that the scaled particle theory model, in which the effective size of the protein's unfolded state to be a linear function of ϕ_c [15], can capture the dependence of the stability enhancement on the crowders' volume fraction at various temperatures.

ACKNOWLEDGMENTS

We thank Ta Thi Quyen for discussions. Nhung T. T. Nguyen was funded by Vingroup JSC and supported by the Postdoctoral Scholarship Programme of Vingroup Innovation Foundation (VINIF), Institute of Big Data, code VINIF.2021.STS.03. T.X.H. acknowledges the support of the Vietnam Academy of Science and Technology for high-level researchers under grant number NVCC05.07/21-21.

REFERENCES

- [1] A. P. Minton, *The effect of volume occupancy upon the thermodynamic activity of proteins: some biochemical consequences*, *Mol. Cell. Biochem.* **55** (1983) 119.
- [2] S. B. Zimmerman and A. P. Minton, *Macromolecular crowding: biochemical, biophysical, and physiological consequences*, *Ann. Rev. Biophys. Biomol. Struct.* **22** (1993) 27.
- [3] H.-X. Zhou, G. Rivas and A. P. Minton, *Macromolecular crowding and confinement: biochemical, biophysical, and potential physiological consequences*, *Annu. Rev. Biophys.* **37** (2008) 375.
- [4] M. S. Cheung, D. Klimov and D. Thirumalai, *Molecular crowding enhances native state stability and refolding rates of globular proteins*, *Proc. Natl. Acad. Sci. USA* **102** (2005) 4753.
- [5] L. Stagg, S.-Q. Zhang, M. S. Cheung and P. Wittung-Stafshede, *Molecular crowding enhances native structure and stability of α/β protein flavodoxin*, *Proc. Natl. Acad. Sci. USA* **104** (2007) 18976.
- [6] B. van den Berg, R. J. Ellis and C. M. Dobson, *Effects of macromolecular crowding on protein folding and aggregation*, *EMBO J.* **18** (1999) 6927.
- [7] I. Horvath, R. Kumar and P. Wittung-Stafshede, *Macromolecular crowding modulates α -synuclein amyloid fiber growth*, *Biophys. J.* **120** (2021) 3374.
- [8] A. P. Minton, *Effect of a concentrated inert macromolecular cosolute on the stability of a globular protein with respect to denaturation by heat and by chaotropes: a statistical-thermodynamic model*, *Biophys. J.* **78** (2000) 101.
- [9] A. P. Minton, *Models for excluded volume interaction between an unfolded protein and rigid macromolecular cosolutes: macromolecular crowding and protein stability revisited*, *Biophys. J.* **88** (2005) 971.
- [10] H.-X. Zhou, *Protein folding in confined and crowded environments*, *Arch. Biochem. Biophys.* **469** (2008) 76.

- [11] A. H. Elcock, *Models of macromolecular crowding effects and the need for quantitative comparisons with experiment*, *Curr. Opin. Struct. Bio.* **20** (2010) 196.
- [12] J. Mittal and R. B. Best, *Dependence of protein folding stability and dynamics on the density and composition of macromolecular crowders*, *Biophys. J.* **98** (2010) 315.
- [13] D. S. Spencer, K. Xu, T. M. Logan and H.-X. Zhou, *Effects of pH, salt, and macromolecular crowding on the stability of fk506-binding protein: an integrated experimental and theoretical study*, *J. Mol. Biol.* **351** (2005) 219.
- [14] A. Roberts and S. E. Jackson, *Destabilised mutants of ubiquitin gain equal stability in crowded solutions*, *Biophys. Chem.* **128** (2007) 140.
- [15] P. T. Bui and T. X. Hoang, *Additive effects of macromolecular crowding and confinement on protein stability*, *Comm. in Phys.* **28** (2018) 351.
- [16] C. Clementi, H. Nymeyer and J. N. Onuchic, *Topological and energetic factors: what determines the structural details of the transition state ensemble and en-route intermediates for protein folding? an investigation for small globular proteins I*, *J. Mol. Biol.* **298** (2000) 937.
- [17] H. Taketomi, Y. Ueda and N. G., *Studies on protein folding, unfolding and fluctuations by computer simulation*, *Int. J. Pep. Protein Res.* **7** (1975) 445.
- [18] P. T. Bui and T. X. Hoang, *Hydrophobic and electrostatic interactions modulate protein escape at the ribosomal exit tunnel*, *Biophys. J.* **120** (2021) 4798.
- [19] Y.-J. Chen, S.-C. Lin, S.-R. Tzeng, H. V. Patel, P.-C. Lyu and J.-W. Cheng, *Stability and folding of the sh3 domain of bruton's tyrosine kinase*, *Proteins: Struct. Funct. Bioinf.* **26** (1996) 465.
- [20] J. W. Brown, J. D. Farelli and C. J. McKnight, *On the unyielding hydrophobic core of villin headpiece*, *Prot. Sci.* **21** (2012) 647.
- [21] P. T. Bui and T. X. Hoang, *Protein escape at the ribosomal exit tunnel: Effects of native interactions, tunnel length, and macromolecular crowding*, *J. Chem. Phys.* **149** (2018) 045102.
- [22] P. T. Bui and T. X. Hoang, *Folding and escape of nascent proteins at ribosomal exit tunnel*, *J. Chem. Phys.* **144** (2016) 095102.
- [23] Y. Sugita and Y. Okamoto, *Replica-exchange molecular dynamics method for protein folding*, *Chem. Phys. Lett.* **314** (1999) 141.
- [24] R. H. Swendsen and J.-S. Wang, *Replica monte carlo simulation of spin-glasses*, *Phys. Rev. Lett.* **57** (1986) 2607.
- [25] A. M. Ferrenberg and R. H. Swendsen, *Optimized monte carlo data analysis*, *Phys. Rev. Lett.* **63** (1989) 1195.
- [26] J. Lebowitz and J. Rowlinson, *Thermodynamic properties of mixtures of hard spheres*, *J. Chem. Phys.* **41** (1964) 133.
- [27] H. Kaya and H. S. Chan, *Polymer principles of protein calorimetric two-state cooperativity*, *Prot. Struct. Func. Bio.* **40** (2000) 637.
- [28] J. Batra, K. Xu, S. Qin and H.-X. Zhou, *Effect of macromolecular crowding on protein binding stability: modest stabilization and significant biological consequences*, *Biophys. J.* **97** (2009) 906.
- [29] A. D. Cunningham, A. Colavin, K. C. Huang and D. Mochly-Rosen, *Coupling between protein stability and catalytic activity determines pathogenicity of g6pd variants*, *Cell Rep.* **18** (2017) 2592.